Designing an intelligent system for vibration diagnosis of centrifugal water-cooling pumps using Bayesian networks

Wiwit Suprihatiningsih[1], Dedik Romahadi[1,2], Aberham Genetu Feleke[2]
[1]Department of Mechanical Engineering, Faculty of Engineering, Universitas Mercu Buana, Jakarta, Indonesia
[2]School of Mechanical Engineering, Beijing Institute of Technology, Beijing, China

Article Info

Article history:

Received Jul 4, 2024
Revised Jul 27, 2025
Accepted Aug 6, 2025

Keywords:

Bayesian networks
Centrifugal pump
Intelligent system
Machine learning
Vibration analysis

ABSTRACT

Implementing monitoring methods is a viable method to reduce substantial damage to cooling water centrifugal pumps. Engaging in manual vibration analysis requires considerable time and a requisite level of competence. Small datasets pose challenges when applying classification systems that utilize linear classification models and deep learning. Given these issues, our proposal entails developing a system capable of autonomously, precisely, and accurately diagnosing vibrations using a limited dataset. The system is anticipated to possess the capability to detect multiple categories of mechanical defects, such as static imbalance, dynamic imbalance, misalignment, cavitation, looseness, and bearing corrosion. The Bayesian network (BN) structure was constructed using the MATLAB software. The input data parameters comprise vibration signals measured in the frequency domain and values representing phase differences. The constructed intelligent system was subsequently assessed using a dataset including 120 samples. The smart system can rapidly anticipate and precisely identify every form of harm with exceptional accuracy and sensitivity, relying on test outcomes. The test data analysis reveals that the intelligent system attained an average accuracy of 94.74%, precision of 95.32%, sensitivity (recall) of 93.67%, and F-score of 94.36%.

Corresponding Author:

Dedik Romahadi
Department of Mechanical Engineering, Faculty of Engineering, Universitas Mercu Buana
Jakarta, Indonesia
Email: dedik.romahadi@mercubuana.ac.id

1. INTRODUCTION

A pump is a device that can move fluid from a higher elevation or an area with lower pressure to a location with higher pressure [1], [2]. The kinetic energy or velocity of the impeller is altered during the pumping process to facilitate its rotation and provide the necessary power for fluid movement [3]. Vibration results from the pump's rotational movement, which causes the impeller, pump shaft, clutch, and other moving parts to rotate. Excessive vibration in the pump can lead to detrimental effects such as shaft and bearing damage, noise generation, decreased head and capacity, and even lower pump efficiency [4]. Utilizing predictive maintenance approaches can help take preventive steps to limit the likelihood of abrupt pump breakdowns. This entails predicting possible engine harm by examining quantifiable parameters and conducting a comprehensive analysis. Vibration analysis is a proactive measure to mitigate excessive vibration in the pump. Vibration can adversely affect a pump's operation, leading to noise, reduced performance, and even harm to critical components like shafts and bearings [5]. Vibration analysis is crucial for predicting damage as it is a significant tool for identifying and detecting mechanical issues. By studying current vibration characteristics, it is possible to evaluate equipment deterioration without disassembly [6], [7].

The most recent iteration of vibration monitoring equipment exhibits enhanced capabilities and automated operations compared to earlier models. Specific devices display an entire vibration spectrum on three axes concurrently, providing a holistic depiction of the operational characteristics of any particular machine. To effectively utilize contemporary vibration measuring systems, it is essential to have a basic understanding of vibration analysis, notwithstanding the numerous technological features and automated functions they offer. Analyzing several parameters in collecting vibration data might provide helpful knowledge of the exact damage inflicted on the equipment. Therefore, doing a thorough analysis can generate suitable recommendations for efficiently handling every occurrence of equipment failure. Several vibration measurements instruments do not possess diagnostic intelligence skills, particularly when classifying damage caused by the imbalance [8], [9]. Users must have a basic comprehension of the fundamentals of vibration analysis concerning different types of structural damage. Even professionals require significant time to diagnose damage caused by imbalance. This is mainly attributed to the constrained functionalities of the existing tools, which generally provide imbalanced damage parameters. Therefore, the user must undertake a sequence of data analysis methods to ascertain the precise nature of the damage that has taken place.

A Bayesian network (BN) is a model that is represented visually, depicting probabilistic interactions between interconnected variables, illustrating causal linkages and dependencies [10]–[12]. BN can offer four distinct methods: BN demonstrates proficiency in properly handling instances of data incompleteness or issues. Moreover, using BNs enables the gathering of knowledge about cause-and-effect correlations. Gaining information and skills is crucial for comprehending the extent of the problem domain. Furthermore, BN can support the amalgamation of domain knowledge and data. Overall, BN offers a scientifically rigorous and efficient approach to mitigate the issue of overfitting in data processing. The process of constructing a model in BN comprises two separate stages: the first step includes establishing the network structure. In contrast, the subsequent steps entail estimating the probability values associated with each node. MATLAB is a software program that enables the construction of BN algorithms. Due to the scarcity of available datasets, the numerous advantages of BN as a decision-making tool, and the endorsement from multiple scientific journals, BN was chosen as the preferred method for creating a diagnostic system for water-cooled centrifugal pump engines [13], [14].

Numerous inquiries have been conducted in this area of research [15]–[17]. Our previous study also discussed the design of an intelligent system to detect types of imbalances by utilizing BN, and satisfactory results were obtained [18]. The damage location can be determined by examining the vibration signal, in which the amplitude of the vibration will be quantified. The results will be displayed in the frequency domain utilizing the fast Fourier transform (FFT) approach. The study conducted by Castellanos *et al.* [3] specifically examined the analysis of vibrations in motors and pumps. The vibration analysis was performed manually using the FFT technology. This method is employed to assess the extent of harm inflicted on the pump, as evidenced by frequency spectrum measurements. Empirical data indicates that harmonic amplitudes measured at whole number multiples of engine speed, precisely at 1, 2, and 3, can be used as a dependable signal for detecting misalignment issues in the presence of variations in motor leg height. In addition, researchers have examined centrifugal pumps utilized in cooling water systems to assess the magnitude of vibration-induced harm. The pump's vibration data is subsequently processed using FFT techniques to enable visual examination and determination of the specific type of damage that has occurred [19]. Analysis of the vibration spectrum indicates the presence of mechanical looseness damage in the motor and pump components. The engine condition assessment is often conducted according to the ISO 10816-3 standard, encompassing speed and acceleration modes. According to data spectrum investigations, the primary cause of damage is rotor imbalance. Within vibration analysis, expert systems prioritize the dependability of BNs in efficiently addressing circumstances that involve uncertainty. The BN method is widely regarded as a practical way to develop intelligent vibration detection applications [20]–[22].

Our proposed research aims to provide a novel approach for constructing a system capable of diagnosing damage to the P-9114B type water cooling centrifugal pump using vibration data. We have developed a method to interpret the root mean square (RMS) as a performance indicator based on the ISO 10816-3 standard. We utilize a novel BN model to analyze the spectrum, enabling it to make determinations based on the specific type of machinery damage. This study yielded a highly efficient approach that can be utilized explicitly for diagnosing pumps. This research aims to aid industry personnel in efficiently and accurately identifying various types of machine damage, even without a comprehensive knowledge of the fundamental principles and ideas of vibration analysis. Researching the utilization of BN to diagnose industrial machinery. The research findings can potentially serve as a basis for establishing a diagnostic system on a broader scale.

2. METHOD

Pump vibration data was obtained through the conduction of vibration measurements. Data was collected using the VibXpert II instrument at both the bearings at the drive end (DE) and the one at the nondrive end (NDE) positions. Measurements were conducted in horizontal, vertical, and axial orientations on both the motor and pump sides. After that, the data processing operation was executed using MATLAB software.

2.1. Vibration data acquisition

Vibxpert II measurement instruments are employed in this investigation to quantify pump vibrations as shown in Figure 1. The instruments used to acquire vibrational data are depicted in Figure 1(a). Table 1 displays the specifications of the Vibxpert II vibration measuring device, while Table 2 displays the specifications of the vibration accelerometer sensor, which are 6.142. For this analysis, we utilized a cooling water centrifugal pump, depicted in Figure 1(b), a crucial element of the cooling tower system. The centrifugal pump, rotating at a speed of 1,450 rpm, has a power output of 114.4 kW. At PT SAU, the fluid is transferred from a cooling tower to a heat exchanger using the P9114B pump. The P9114B DE pump utilizes a 3314-type angular contact bearing, while the NDE and DE-NDE motor side utilizes a ball cushion in the 6314-type groove. The gland packing kind is used to seal asbestos rather than provide lubrication. The specs for the P9114B centrifugal cooling water pump are displayed in Table 3.

(a) (b)

Figure 1. Vibration measurement setup of centrifugal pump P9114B, (a) VibXpert II data collector with sensor 6.142 used for vibration analysis and (b) centrifugal pump with labeled measurement points at DE-NDE motor and pump

Table 1. VibXpert II specification

Name	Specification
Range frequency	0.5 Hz–40 kHz
Environment protection	IP65
Temperature operational	0-50 °C
Data memori	128 MB DDR RAM
Tipe baterai	Li-ion *rechargeable* (7.3 V/5.3 Ah–38.7 Wh)
Dimension	186×162×52 mm (LxWxH)

Table 2. Vibration sensor specification

Name	Specification
Transmision factor	1.0 µA/m/s^2
Resonance frequency	36 kHz
Temperature range	-40-100 °C
Case material	Stainless steel VA 1.4305
Environment protection	IP 65

Table 3. Centrifugal pump P9114B specification

Name	Specification
Pump type	Centrifugal pump
Model	3K 10 X 8-16/156
Brand	DURCO MARK III
Suction pressure	5.5 Bar
RPM	1,450
Power	114.4 kW

2.2. Primary fault frequency component

Frequency requirements and computations are crucial in investigating machine failure, particularly bearing frequencies [23]. The pump utilizes type 6,314 ball bearings and is accompanied by comprehensive specifications. In (1) to (4) display the frequencies specific to different bearing components, such as the inner and outer races, balls or rollers, and cages. If a bearing element frequency is confirmed, it signifies a bearing issue associated with pump damage. In (1) can be used to calculate the frequency of ball passes frequency in the inner ring (BPFI).

$$BPFI = \frac{RPM}{120}\left(1 + \frac{D_B}{D_P} cos\, \beta\right) \tag{1}$$

Where D_B is a ball diameter of 20 mm, D_P is a pitch diameter of 100 mm, β In this case, the contact angle is 0º, and the motor centrifugal pump speed is 1,450 rpm or 24.17 Hz. In (2) can be used to determine the outer ring's ball pass frequency outer (BPFO).

$$BPFO = \frac{RPM}{120}\left(1 + \frac{D_B}{D_P} cos\, \beta\right) \cdot N_B \tag{2}$$

Where N_B is the number of ball bearings equal to 8 ball bearings. Fundamental train frequency (FTF) is calculated using (3).

$$FTF = \frac{RPM}{120}\left(1 - \frac{D_B}{D_P} cos\, \beta\right) \tag{3}$$

Meanwhile, ball spin frequency (BSF) can be obtained from (4).

$$BSF = \frac{RPM}{120}\left(1 - \left(\frac{D_B}{D_P} cos\, \beta\right)^2\right) \cdot \frac{D_P}{D_B} \tag{4}$$

The centrifugal pump impeller has six blade angles. Use (5) to compute the frequency generated by the pump impeller, i.e., ball pass frequency (BPF).

$$BPF = \frac{B_N}{60} \times RPM \tag{5}$$

In addition to the frequencies mentioned in (1) to (5), another significant frequency is the one associated with motor spinning. The motor rotation frequency of 21.17 Hz is commonly referred to as 1X and can also be referred to as multiples, such as 2X, 3X, and so forth.

2.3. Vibration assessment

The time domain vibration data is obtained using the RMS approach, as in (6) [24]. The findings of the RMS computation will be compared against the ISO 10816-3 standard. This study aims to assess the pump's magnitude and state of vibration. ISO 10816, as referenced in [25], outlines standards for evaluating when taking readings of vibration levels directly at the measurement site.

$$x_{RMS} = \sqrt{\frac{1}{N}\sum_{n=1}^{N}|x_n|^2} \tag{6}$$

The above criteria pertain to machine devices with a power rating exceeding 15 kW and an operational speed ranging from 120 to 15,000 revolutions per minute. The ISO 10816-3:2009 standard, based on velocity measurements, evaluates the vibration levels in machines with a rotating speed exceeding 600 rpm. Vibration assessment typically uses units of mm/s RMS. Suppose the RMS value is under the specified limit of 4.5 mm/s, as stated in the ISO 10816-3 group 2 standard for a rigid foundation type. In that case, the vibration level of the pump is considered acceptable. Therefore, there is no need to continue with the subsequent procedure. However, if the vibration surpasses 4.5 mm/s, it is necessary to examine and identify the origin of the damage.

2.4. System flowchart

Figure 2 depicts a detailed flowchart illustrating the flow of a particular system. The BN method will calculate the probability value using the input data. This process involves several stages, including solving for each damage symptom by finding its parameter value and calculating the probability value under certain conditions. Once the data is collected, the algorithm will determine the combined and posterior probability value for every form of damage. The BN framework is changed, and the posterior probability estimation is utilized to make a probability inference regarding the damage. BN utilizes two-way propagation between nodes that receive and send data to provide relational information and conditional probabilities. In practical applications, multistate nodes are commonly used. Based on the user's consultation, they will receive information on the specific damage to the machine and the percentage of errors.

Users are required to compile data in the format of machine specs and vibration data. The system will analyze the numbers that make up the vibration spectrum to generate information whose output the BN can utilize. The provided spectrum data is further analyzed to determine the frequency of each machine component. The details about the machine's specifications will be a reference for frequency calculations and will be fine-tuned to match the spectrum. If the computed frequency value is present in the spectrum, it will serve as evidence for BN. Conversely, if the frequency value is not found in the spectrum, it will not provide any proof of JB. JB's input data is categorized into two distinct kinds. Frequency lines empirically verified by frequency calculation are classified as input type 1 (true). This input requires that the frequency amplitude be equal to or greater than 2 mm/s RMS. However, if the data does not contain a frequency line supported by the computation or a frequency amplitude value of less than 2 mm/s RMS, it is classified as input type 2 (false).

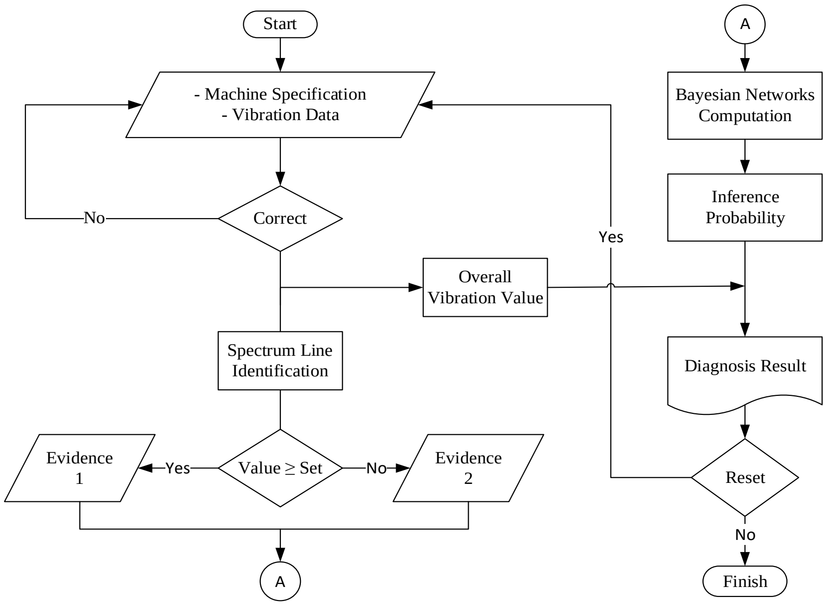

Figure 2. System flowchart

2.5. System performance calculations

Assessment is conducted within the framework of supervised learning. As the literature illustrates, each matrix row denotes an actual class occurrence, while each column denotes a predicted class occurrence. An alternative structure proposed in the academic literature entails the alignment of each row with anticipated class events and each column with actual class events. This nomenclature aims to enhance the identification process if the system inaccurately assigns the same category to two distinct groups, frequently leading to misclassification. The examined contingency table comprises two dimensions: "actual" and "predicted." Both dimensions encompass identical "classes." Each variable in a contingency table is a distinctive combination of classifications and dimensions. A true positive (TP) is a situation in which the actual value and the prediction are both positive. A true negative (TN) is a situation in which both the precise number and the prediction are negative. A false positive (FP) is a situation in which the prediction is positive, even though the truth is negative. It is also referred to as a type 1 error. A false negative (FN) is a situation in which the truth is positive, but the prediction is negative. It is also referred to as a type 2 error.

System performance is evaluated by calculating accuracy, precision, sensitivity (or recall), specificity, and F-score. In (7) can be used to calculate the precision of the system's prediction findings:

$$Accuracy = \frac{TP+TN}{TP+TN+FP+FN} \tag{7}$$

In (8) is used to determine the system's performance, which is expressed as the recall value or sensitivity.

$$Sensitivity = \frac{TP}{TP+FN} \tag{8}$$

Determine the system's precision in forecasting the specific type of machine damage by utilizing (9).

$$Precision = \frac{TP}{TP+FP} \tag{9}$$

The specificity parameters and F-score are computed using (10) and (11), respectively.

$$Specificity = \frac{TN}{TN+FP} \tag{10}$$

$$\text{F-}score = \frac{2TP}{2TP+FP+FN} \tag{11}$$

3. RESULTS AND DISCUSSION

This intelligent system specifically intends to detect vibrations in centrifugal pumps by analyzing spectrum data. This can potentially minimize the requirement for professional individuals to be involved in the diagnosis process. A sophisticated technique was developed to detect centrifugal vibrations by examining frequency lines in the spectrum using a pre-established knowledge base. Users can efficiently and effortlessly access sophisticated systems to ascertain centrifuge conditions promptly.

3.1. Test data collection of measurement results

The intelligent system underwent testing utilizing training data, including spectrum data, DE-NDE phase bearing differences, and vertical horizontal phase differences. The test data comprises 20 sets, each containing misalignment damage data, static unbalanced damage data, dynamic unbalanced damage data, looseness damage data, cavitation damage data, and bearing damage data. A maximum of 120 samples can be gathered to evaluate the efficacy of the developed intelligent system application. Test data generation involves utilizing pump frequency values, bearing frequency values, BFP frequency values, vibration diagnosis charts, and ISO 10816-13 [25]. In addition, test data were gathered from the P911B cooling water pump. Here are some examples of spectrum data used for testing intelligent systems. Figure 3 shows the fault indication of FFT results, Figure 3(a) depicts a spectrum data graph illustrating the effects of imbalance damage. The graph indicates a significant magnitude at a frequency of 24.17 Hz, corresponding to one revolution per minute of the centrifugal pump. According to sources, single high amplitude is distinguishing feature of unbalanced damage.

Figure 3(b) presents a spectral data graph that demonstrates the occurrence of cavitation damage. The graph displays a conspicuous peak with a large magnitude at a frequency of 145 Hz, six times the rotational speed or frequency at which the blades of a centrifugal pump pass by. The graph illustrates that cavitation damage in centrifugal pumps is characterized by a significant amplitude at 6 times the revolutions per minute (RPM). Figure 3(c) presents a spectrum graph illustrating the extent of damage to the looseness of the bearing housing or foundation. The graph exhibits notable peaks at 12.08, 24.17, 48.33, and 72.5 Hz. The frequencies are 0.5, 1, 2, and 3 times the RPM. An elevated peak in this frequency signifies an issue with the foundation or bearing. The presence of significant peaks at 1X, 2X, and 3X values suggests the existence of misalignment issues [23], [26], [27]. Figure 3(d) presents a spectrogram illustrating the presence of bearing damage. The graph exhibits notable peaks at 9.67, 58, 72.5, and 115.97 Hz frequencies. The frequencies mentioned are FTF, BSF, BPFO, and BPFI. If the magnitude of any of the FTF, BSF, BPFO, or BPFI increases significantly, it suggests a problem with the bearing [23].

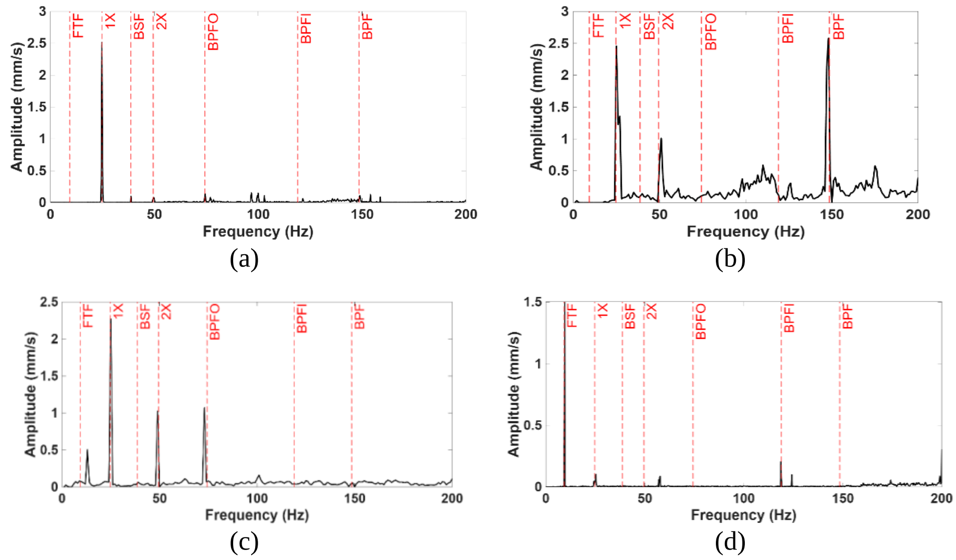

Figure 3. Fault indication of FFT results of (a) unbalance, (b) cavitation, (c) looseness, and (d) bearing

3.2. Bayesian network modeling

The design outcomes of the BN will serve as a benchmark for developing intelligent system applications, as depicted in Figure 4. The BN is structured on three hierarchical layers. The initial stage comprises a set of characteristics that result in detrimental effects on the pump. The following is a clarification provided in Table 4. The second-level arrangement comprises the factors that result in harm, which are the same parameters that produce damage at level 1. Table 5 depicts the organization at the second level. Additionally, the second level is determined using vibration diagnostics, which analyzes the characteristics responsible for the damage identified in both the first and second levels, as outlined in Table 6.

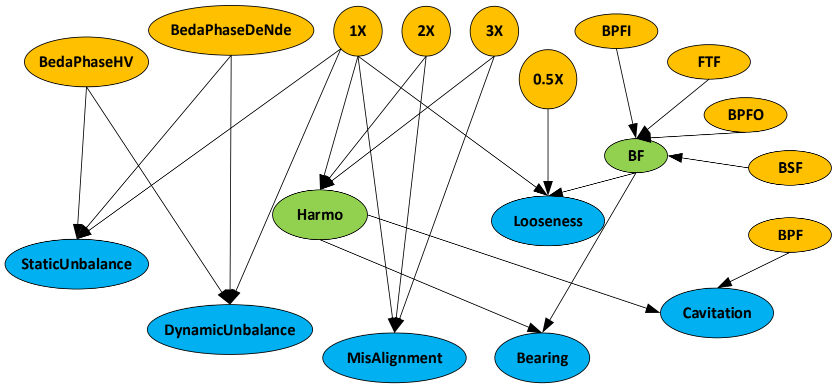

Figure 4. BN architecture

Table 4. Prior probability

Node	Description
1X	When the amplitude is large, and the frequency is 1X
2X	When the amplitude is large, and the frequency is 2X
3X	When the amplitude is large, and the frequency is 3X
0.5X	When the amplitude is large, and the frequency is 0.5X
Beda*Phase*HV	Different phase bearings DE and NDE
Beda*Phase*DeNde	Different horizontal and vertical phases
BPFI	Occurs when the magnitude is elevated at the BPFI frequency
BPFO	Occurs when the magnitude is elevated at the BPFO frequency
BSF	Occurs when the magnitude is elevated at the BSF frequency
FTF	Occurs when the magnitude is elevated at the FTF frequency
BPF	Occurs when the magnitude is elevated at the BPF frequency

Table 5. Conditional probability 1

Node	Description
Harmo	Harmonics with parameters 1X, 2X, 3X
BF	Bearing Frequency with symptoms of BPFI, BPFO, BSF, FTF

Table 1. Conditional probability 2

Node	Parameter
Staticunbalance	Beda*Phase*HV, Beda*Phase*DeNde, 1X, Conditional
Dynamicunbalance	Beda*Phase*HV, Beda*Phase*DeNde, 1X, Conditional
Misalingment	1X, 2X, 3X, Conditional
Looseness	0.5X, 1X, Harmo
Bearing	Harmo, BF
Cavitation	Harmo, BPF

3.3. Recognition of input data

The intelligent system identifies input data values by establishing their value boundaries, including the overall vibration value in RMS, frequency spectrum data, DE NDE phase difference values, and horizontal and vertical phase difference values. The RMS value assesses the pump's condition according to ISO 10816-3. Table 7 provides a comprehensive record of the vibration levels observed in centrifugal pumps. The frequency spectrum data identification process is employed to analyze amplitude values and extract frequency data values, such as 1X, 2X, 3X, 0.5X, BPF, and bearing frequencies. The damage to the centrifugal pump can be determined by calculating the prior probability and conditional probability based on the identified frequency. Table 8 contains the specifications for identifying vibration spectrum data. The minimal value indicates that the system will not generate evidence for BN unless the amplitude surpasses the specified minimum threshold, as outlined in Table 8.

Table 7. Overall vibration assessment

Overall Vibration Value in RMS	Machine condition
0 mm/s to <=1.4 mm/s	Good condition
>1.4 mm/s to <=2.8 mm/s	Long-term operation is still permitted
>2.8 mm/s to <=4.5 mm/s	Short-term operation is still permitted
>4.5 mm/s	Stop operation; vibration will cause damage

Table 8. Vibration spectrum data assessment

Frequency (Hz)	Minimum amplitude (mm/s)
1X (24.17)	2
2X (48.33)	1
3X (72.50)	1
0.5X (12.08)	0.5
BPFI (115.97)	0.3
BPFO (77.31)	0.3
BSF (58)	0.3
FTF (9.66)	0.3
BPF (9.66)	0.5

3.4. Different phase DE-NDE and H-V assessment

The identification of DE NDE phase difference values and horizontal and vertical phase differences is used to ascertain static and dynamic unbalance. If the phase difference between the DE and NDE is within the range of 0º±30º, it indicates the presence of static unbalance. If the disparity between the DE and NDE is greater than 30º, it suggests the presence of dynamic unbalance. A phase difference of 90º±30º between the vertical and horizontal sides of the bearing indicates a significant likelihood of imbalance. A phase difference between the vertical and horizontal sides of the bearing that falls outside the range of 90º±30º suggests a low probability of imbalance damage.

3.5. Bayesian network probability

The Microsoft belief network generates probabilities, serving as a framework for developing intelligent system applications with MATLAB. Probability is derived from the conditional probability table (CPT). The CPT displays the likelihood of a specific condition happening, given that certain conditions are satisfied. The probability of diagnosing vibration in centrifugal pumps can be shown in Tables 9 to 13. Table 9 displays the CPT of static unbalanced damage. The P9114B cooling water pump damage caused by static unbalance is affected by the phase discrepancies between the DE and NDE, both horizontally and vertically, and by high amplitude at a particular frequency. The greatest likelihood occurs when the difference in phase between DE and NDE and the difference in phase between H and V are constant, and there is a significant amplitude at the frequency of 1X, provided that the amplitude at 1X is larger than at 2X.

Table 11 presents the CPT results for looseness damage. The damage caused by looseness in centrifugal pumps is affected by harmonic waves, particularly those with high amplitude at 0.5 and 1 time the main frequency. The greatest likelihood occurs when harmonic waves (Harmo) have a high amplitude at frequencies of 0.5X and 1X. The CPT for misalignment damage is displayed in Table 11. Misalignment damage in centrifugal pumps is distinguished by significant amplitudes occurring at the fundamental frequency and its harmonics, including twice and three times the frequency. Additionally, there are conditional factors that might influence the extent of the damage. The maximum likelihood occurs when the amplitude is elevated at frequencies of 1X, 2X, and 3X, with the amplitude at 1X being smaller than that at 2X. Table 12 displays the CPT (cavitation damage) values. The extent of cavitation damage to machines is determined by the high amplitude of the pump's BPF and harmonic waves. The maximum likelihood occurs when the amplitude is elevated at the bandpass filter's frequency, and several harmonic waves are present. Table 13 displays the CPT for bearing failure. The occurrence of bearing damage in centrifugal pumps is affected by high amplitudes of specific bearing frequencies, particularly BPFI, BPFO, BSF, FTF, and harmonic waves. The maximum likelihood occurs when the amplitude is elevated at the frequency associated with the bearing and other harmonic waves are present.

Table 9. Probability of dynamic unbalance

<table>
<tr><th colspan="2">Parent node(s)</th><th colspan="4">Dynamic unbalance</th></tr>
<tr><th>BedaPhaseDeNde</th><th>BedaPhaseHV</th><th>1X</th><th>Yes</th><th>No</th><th>Bar charts</th></tr>
<tr><td>Static</td><td>Static</td><td>Yes</td><td>0.3</td><td>0.7</td><td>||||||||||||</td></tr>
<tr><td></td><td></td><td>No</td><td>0.1</td><td>0.9</td><td>||||</td></tr>
<tr><td></td><td>Dynamic</td><td>Yes</td><td>0.7</td><td>0.3</td><td>||||||||||||||||||||||||||||</td></tr>
<tr><td></td><td></td><td>No</td><td>0.2</td><td>0.8</td><td>||||||||</td></tr>
<tr><td>Dynamic</td><td>Static</td><td>Yes</td><td>0.7</td><td>0.3</td><td>||||||||||||||||||||||||||||</td></tr>
<tr><td></td><td></td><td>No</td><td>0.2</td><td>0.8</td><td>||||||||</td></tr>
<tr><td></td><td>Dynamic</td><td>Yes</td><td>0.9</td><td>0.1</td><td>||||||||||||||||||||||||||||||||||||</td></tr>
<tr><td></td><td></td><td>No</td><td>0.3</td><td>0.7</td><td>||||||||||||</td></tr>
</table>

Table 10. Probability of looseness

<table>
<tr><th colspan="3">Parent node(s)</th><th colspan="3">Misalignment</th></tr>
<tr><th>1X</th><th>2X</th><th>3X</th><th>Yes</th><th>No</th><th>Bar charts</th></tr>
<tr><td>Yes</td><td>Yes</td><td>Yes</td><td>0.95</td><td>0.05</td><td>||||||||||||||||||||||||||||||||||||||</td></tr>
<tr><td></td><td></td><td>No</td><td>0.85</td><td>0.15</td><td>||||||||||||||||||||||||||||||||||</td></tr>
<tr><td></td><td>No</td><td>Yes</td><td>0.7</td><td>0.3</td><td>||||||||||||||||||||||||||||</td></tr>
<tr><td></td><td></td><td>No</td><td>0.1</td><td>0.9</td><td>||||</td></tr>
<tr><td>No</td><td>Yes</td><td>Yes</td><td>0.3</td><td>0.7</td><td>||||||||||||</td></tr>
<tr><td></td><td></td><td>No</td><td>0.1</td><td>0.9</td><td>||||</td></tr>
<tr><td></td><td>No</td><td>Yes</td><td>0.1</td><td>0.9</td><td>||||</td></tr>
<tr><td></td><td></td><td>No</td><td>0.0</td><td>1.0</td><td></td></tr>
</table>

Table 11. Probability of misalignment

<table>
<tr><th colspan="3">Parent node(s)</th><th colspan="3">Misalignment</th></tr>
<tr><th>1X</th><th>2X</th><th>3X</th><th>Yes</th><th>No</th><th>Bar charts</th></tr>
<tr><td>Yes</td><td>Yes</td><td>Yes</td><td>0.95</td><td>0.05</td><td>||||||||||||||||||||||||||||||||||||||</td></tr>
<tr><td></td><td></td><td>No</td><td>0.85</td><td>0.15</td><td>||||||||||||||||||||||||||||||||||</td></tr>
<tr><td></td><td>No</td><td>Yes</td><td>0.7</td><td>0.3</td><td>||||||||||||||||||||||||||||</td></tr>
<tr><td></td><td></td><td>No</td><td>0.1</td><td>0.9</td><td>||||</td></tr>
<tr><td>No</td><td>Yes</td><td>Yes</td><td>0.3</td><td>0.7</td><td>||||||||||||</td></tr>
<tr><td></td><td></td><td>No</td><td>0.1</td><td>0.9</td><td>||||</td></tr>
<tr><td></td><td>No</td><td>Yes</td><td>0.1</td><td>0.9</td><td>||||</td></tr>
<tr><td></td><td></td><td>No</td><td>0.0</td><td>1.0</td><td></td></tr>
</table>

Table 12. Probability of cavitation

<table>
<tr><th colspan="2">Parent node(s)</th><th colspan="3">Cavitation</th></tr>
<tr><th>BPF</th><th>Harmo</th><th>Yes</th><th>No.</th><th>Bar charts</th></tr>
<tr><td>Yes</td><td>Yes</td><td>0.9</td><td>0.1</td><td>||||||||||||||||||||||||||||||||||||</td></tr>
<tr><td></td><td>No.</td><td>0.85</td><td>0.15</td><td>||||||||||||||||||||||||||||||||||</td></tr>
<tr><td>No.</td><td>Yes</td><td>0.4</td><td>0.6</td><td>||||||||||||||||</td></tr>
<tr><td></td><td>No.</td><td>0.1</td><td>0.9</td><td>||||</td></tr>
</table>

Table 13. Probability of bearing

<table>
<tr><th colspan="2">Parent node(s)</th><th colspan="3">Bearing</th></tr>
<tr><th>Harmo</th><th>BF</th><th>Yes</th><th>No</th><th>Bar charts</th></tr>
<tr><td>Yes</td><td>Yes</td><td>1.0</td><td>0.0</td><td>||||||||||||||||||||||||||||||||||||||||</td></tr>
<tr><td></td><td>No</td><td>0.3</td><td>0.7</td><td>||||||||||||</td></tr>
<tr><td>No</td><td>Yes</td><td>0.95</td><td>0.05</td><td>||||||||||||||||||||||||||||||||||||||</td></tr>
<tr><td></td><td>No</td><td>0.0</td><td>1.0</td><td></td></tr>
</table>

3.6. Intelligent system design results

The construction of an intelligent system application commences by integrating a program that allows input of data values and damage probabilities. Programming is conducted within the Live Editor submenu of the MATLAB software. The application's user interface includes instructions for using the application, a spectrum graph panel for displaying the frequency spectrum, an input data panel, a panel for displaying diagnosis results for failure types that occur more than 50% of the time based on the entered input data, and a machine condition panel that shows the machine's condition based on the RMS value. Upon entry, a graph illustrating the likelihood of failure is presented, depicting the percentage probability of damage or malfunction. The application also contains multiple command buttons. The insert spectrum button inputs vibration spectrum data. The start button initiates the diagnosis procedure. The reset button restores the intelligent system application to its original state, as depicted in Figure 5.

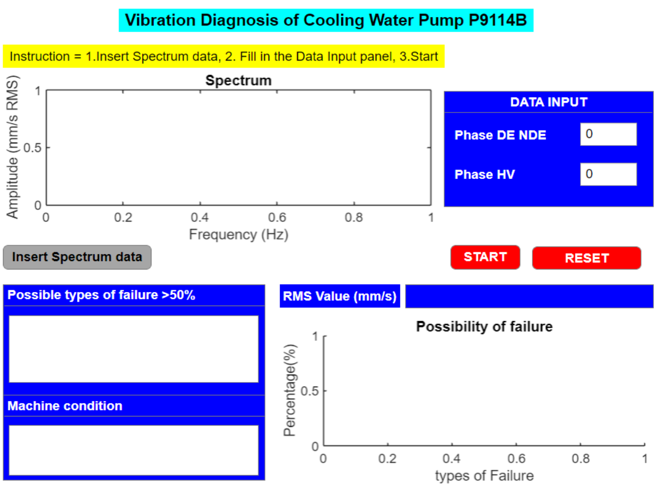

Figure 5. Intelligent system application display

3.7. System test results

Once the intelligent system design is finished, the subsequent stage involves testing the developed intelligent system application. Intelligent system application testing is conducted to verify that the system developed aligns with the references, analysis, and design outcomes. Within this phase, comprehensive testing will be conducted on each variant of damaged input data. Subsequently, the diagnostic outcomes generated by the intelligent system application will be juxtaposed with the manual diagnosis, enabling the assessment of the efficacy of the developed system. Twenty tests were conducted for each type of damage, using different spectrum variants, overall vibration values, DE-NDE phase difference values, and horizontal-vertical phase values. The objective of conducting diverse testing is to assess the efficiency of the intelligent system application under different types of damage scenarios on the P911B cooling water centrifugal pump.

Figure 6 shows a graph displaying testing using input data on dynamic unbalanced damage. The input data consists of an RMS value of 4.39 mm/s, a DE NDE phase of 83º, a vertical-horizontal phase of 140º, and a frequency spectrum with high amplitude at 1 rpm. The system generates a diagnosis indicating a dynamic unbalanced problem with a 90% likelihood and allows for short-term operational recommendations. Testing was carried out to verify that the intelligent system was operating according to its design and to evaluate the performance of the smart system in diagnosing the condition of the centrifugal pump. Testing of the intelligent system produced 120 data. After testing is complete, the data is analyzed to evaluate the quality of the smart system that has been created. The test results were processed with the help of the confusion matrix method, as seen in Figure 7.

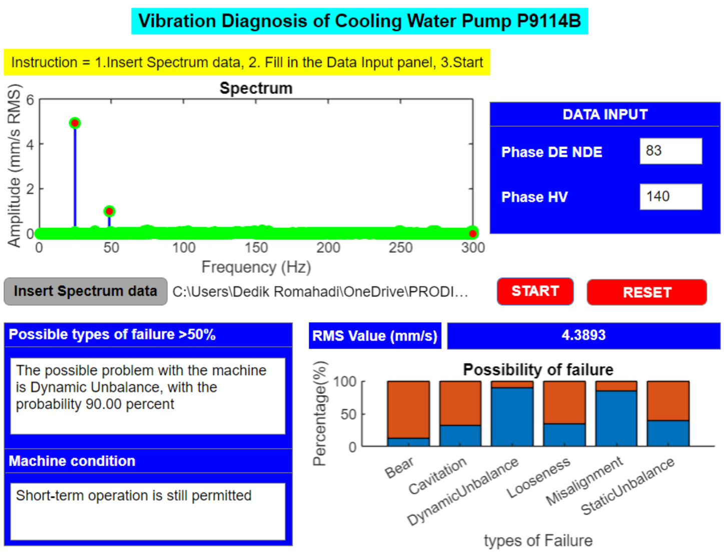

Figure 6. Intelligent diagnosis model testing output for a cooling-water centrifugal pump

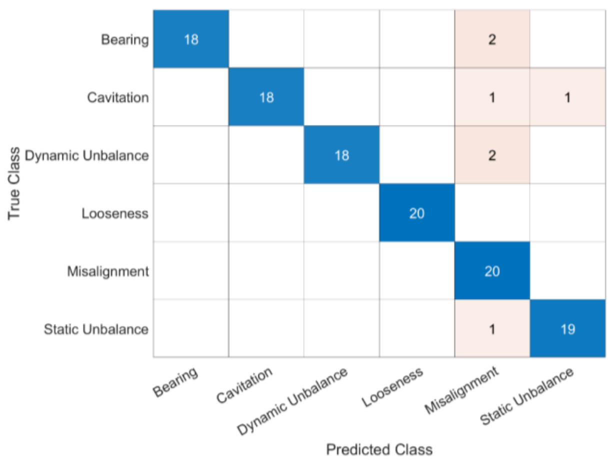

Figure 7. Confusion-matrix evaluation of the proposed fault-diagnosis model on the test set (n=120)

The x-axis represents the actual diagnosis outcome, while the y-axis represents the predicted harm from the intelligent system. In the initial assessment of the intelligent system's capability to detect bearing damage, it accurately diagnosed the issue (TP) 18 times and incorrectly diagnosed it (FN) 2 times. The intelligent system achieved an accuracy rate of 18 actual positive diagnoses and 2 FN diagnoses in detecting cavitation damage. The intelligent system accurately identified dynamic unbalanced damage in 18 instances (TP) and made incorrect diagnoses in two cases (FN). The clever technology has a diagnostic accuracy of 20 times the rate of correctly identifying looseness damage (TP). The intelligent system accurately identifies misalignment in the test data 20 times (TP) and incorrectly identifies misalignment damage in other data (FP) 6 times. The intelligent system accurately diagnoses static imbalance damage 19 times (TP), incorrectly diagnoses it once (FN), and misdiagnoses other types of damage once (FP).

The specifics and computed outcomes of the confusion matrix graph can be seen in Table 14. The TP column represents the intelligent system's accuracy in properly diagnosing 20 instances of damage in the test data. In the table, the highest values occur 20 times for looseness and misalignment, while the lowest values occur for bearings, cavitation, and dynamic unbalance, each appearing 18 times. The term "TN" refers to the total number of test data points that do not pertain to the specific type of damage being tested. An FP occurs when the intelligent system incorrectly identifies a certain kind of damage in other test data as damage. In the misalignment table, it has the most occurrences, 6 times, followed by static imbalance, which occurs once. An FN occurs when the intelligent system incorrectly diagnoses damage based on the test data provided. The table displays the maximum values for bearing, cavitation, and dynamic unbalance, each occurring twice. Conversely, the lowest values are for misalignment and looseness, with a value of 0.

The intelligent system demonstrates a diagnostic accuracy of 100% for identifying looseness and misalignment, while it achieves a lower accuracy of 94.17% for detecting bearing issues, cavitation, dynamic unbalance, and static unbalance. The intelligent system exhibits exceptional precision levels of 100% in bearing, cavitation, dynamic unbalance, and looseness. However, it demonstrates a relatively lower precision of 76.92% in detecting misalignment, which can be attributed to the system requesting data on other types of damage on six occasions. The recall or sensitivity rates were highest for looseness and misalignment, at 100%, and the lowest percentage for misalignment, at 76.92%. The F-score is an alternative to accuracy when the values of FP and FN significantly differ. In the F-score table, the highest value represents a 100% tolerance, while the lowest value indicates a misalignment of 86.96%. Analysis of the test data revealed that the intelligent system exhibited an average accuracy of 94.74%, precision of 95.32%, sensitivity (recall) of 93.67%, and an F-score of 94.36%.

Table 14. BN performance

Name	Classes					
	Bearing	Cavitation	Dynamic unbalance	Looseness	Misalignment	Static unbalance
TN	100	100	100	100	94	99
FP	0	0	0	0	6	1
FN	2	2	2	0	0	1
TP	18	18	18	20	20	19
Precision	1	1	1	1	0.7692	0.95
Sensitivity	0.9	0.9	0.9	1	1	0.95
Specificity	1	1	1	1	0.94	0.99
Accuracy	0.9417	0.9417	0.9417	0.9417	0.9417	0.9417
F-score	0.9474	0.9474	0.9474	1	0.8696	0.95

4. CONCLUSION

The developed intelligent system can rapidly diagnose the condition of the P911B cooling water centrifugal pump using a reference-based approach. A sophisticated approach was created utilizing vibration diagnosis charts to accurately determine the specific damage type. At the same time, ISO 10816-3 was employed to evaluate the overall condition of the P911B cooling water pump. The BN is formed using the diagnosis reference graph. A BN comprises input and output nodes that reflect misalignment, static imbalance, dynamic imbalance, looseness, and cavitation. Testing shall consist of 20 sets of test data, each containing diverse variations for every damage category. The intelligent system can rapidly anticipate and precisely identify each form of harm with exceptional accuracy and sensitivity, relying on test outcomes. The examination of the test data reveals that the intelligent system attained an average accuracy of 94.74%, precision of 95.32%, sensitivity (recall) of 93.67%, and F-score of 94.36%.

FUNDING INFORMATION

This research was funded by Universitas Mercu Buana through the IKU Domestic Cooperation Research Scheme under contract No. 02-5/216/B-SPK/II/2024.

AUTHOR CONTRIBUTIONS STATEMENT

This journal uses the Contributor Roles Taxonomy (CRediT) to recognize individual author contributions, reduce authorship disputes, and facilitate collaboration.

Name of Author	C	M	So	Va	Fo	I	R	D	O	E	Vi	Su	P	Fu
Wiwit Suprihatiningsih	✓				✓				✓		✓		✓	✓
Dedik Romahadi		✓	✓	✓		✓	✓	✓		✓		✓		
Aberham Genetu Feleke	✓	✓				✓				✓		✓		

C : **C**onceptualization
M : **M**ethodology
So : **So**ftware
Va : **Va**lidation
Fo : **Fo**rmal analysis
I : **I**nvestigation
R : **R**esources
D : **D**ata Curation
O : Writing - **O**riginal Draft
E : Writing - Review & **E**diting
Vi : **Vi**sualization
Su : **Su**pervision
P : **P**roject administration
Fu : **Fu**nding acquisition

CONFLICT OF INTEREST STATEMENT

The authors declare that they have no financial interests or personal relationships that could be interpreted as having influenced the research reported in this paper.

DATA AVAILABILITY

The data that support the findings of this study are available on request from the corresponding author, [DR]. The data, which contain information that could compromise the privacy of research participants, are not publicly available due to certain restrictions.

REFERENCES

[1] A. R. A.-Obaidi, “Investigation of effect of pump rotational speed on performance and detection of cavitation within a centrifugal pump using vibration analysis,” *Heliyon*, vol. 5, no. 6, 2019, doi: 10.1016/j.heliyon.2019.e01910.
[2] D. Nusraningrum, A. R. Rachmat, Z. Y. Tan, W. Wider, L. Jiang, and N. Hongsrisuwan, “Qualitative evaluation and corrective planning for centrifugal pump maintenance at Soekarno-Hatta airport,” *Journal of Infrastructure, Policy and Development*, vol. 8, no. 12, 2024, doi: 10.24294/jipd.v8i12.6228.
[3] M. B. Castellanos, F. d. C. T. Carvalho, J. L. Biazussi, and A. L. Serpa, “Phase inversion identification in electrical submersible pumps using mechanical vibrations,” *Flow Measurement and Instrumentation*, vol. 93, 2023, doi: 10.1016/j.flowmeasinst.2023.102419.
[4] X. Yang, J. Lian, Z. Zhang, and Y. Zeng, “Theoretical analysis of the attenuation characteristics of high-frequency pressure vibration in pumped storage power station,” *Journal of Energy Storage*, vol. 72, 2023, doi: 10.1016/j.est.2023.108341.
[5] J. Lian, X. Yang, and H. Wang, “Propagation characteristics analysis of high-frequency vibration in pumped storage power station based on a 1D fluid-solid coupling model,” *Journal of Energy Storage*, vol. 68, 2023, doi: 10.1016/j.est.2023.107869.
[6] H. Pang, D. Wu, Y. Deng, Q. Cheng, and Y. Liu, “Effect of working medium on the noise and vibration characteristics of water hydraulic axial piston pump,” *Applied Acoustics*, vol. 183, 2021, doi: 10.1016/j.apacoust.2021.108277.
[7] J. P. S. Gonçalves, F. Fruett, J. G. D. Filho, and M. Giesbrecht, “Faults detection and classification in a centrifugal pump from vibration data using Markov parameters,” *Mechanical Systems and Signal Processing*, vol. 158, 2021, doi: 10.1016/j.ymssp.2021.107694.
[8] H. Miao, C. Wang, C. Li, W. Song, X. Zhang, and M. Xu, “Nonlinear dynamic modeling and vibration analysis of whole machine tool,” *International Journal of Mechanical Sciences*, vol. 245, 2023, doi: 10.1016/j.ijmecsci.2023.108122.
[9] K. Gomathi and A. Balaji, “Tool condition monitoring of PCB milling machine based on vibration analysis,” *Materials Today: Proceedings*, vol. 45, pp. 3386–3397, 2021, doi: 10.1016/j.matpr.2020.12.778.
[10] S. Pérez, C. G.-Labaume, S. Mathiot, S. Goix, and P. Chamaret, “Using Bayesian networks for environmental health risk assessment,” *Environmental Research*, vol. 204, 2022, doi: 10.1016/j.envres.2021.112059.
[11] P. Xu, J. Chen, J. Li, S. Fan, and Q. Xu, “Using Bayesian updating for monopile offshore wind turbines monitoring,” *Ocean Engineering*, vol. 280, 2023, doi: 10.1016/j.oceaneng.2023.114801.
[12] B. Sun, Y. Li, Z. Wang, D. Yang, Y. Ren, and Q. Feng, “A combined physics of failure and Bayesian network reliability analysis method for complex electronic systems,” *Process Safety and Environmental Protection*, vol. 148, pp. 698–710, 2021, doi: 10.1016/j.psep.2021.01.023.
[13] A. H. d. A. Melani, M. A. d. C. Michalski, R. F. d. Silva, and G. F. M. d. Souza, “A framework to automate fault detection and diagnosis based on moving window principal component analysis and Bayesian network,” *Reliability Engineering and System Safety*, vol. 215, 2021, doi: 10.1016/j.ress.2021.107837.
[14] G. R. Taira, S. W. Park, A. C. Zanin, and C. R. Porfirio, “Fault detection in a fluid catalytic cracking process using Bayesian recurrent neural network,” *IFAC-PapersOnLine*, vol. 55, no. 7, pp. 715–720, 2022, doi: 10.1016/j.ifacol.2022.07.528.
[15] D. F. Plöger, P. Zech, and S. Rinderknecht, “Vibration signature analysis of commodity planetary gearboxes,” *Mechanical Systems and Signal Processing*, vol. 119, pp. 255–265, 2019, doi: 10.1016/j.ymssp.2018.09.014.
[16] N. Nicusor, L. Baicu, and B. Dumitrascu, “Vibration spectrum analysis using FFT in the microcontroller,” in *2022 IEEE 28th International Symposium for Design and Technology in Electronic Packaging, SIITME 2022*, 2022, pp. 176–180, doi: 10.1109/SIITME56728.2022.9987820.
[17] M. d. R. B.-Morales and L. D. P.-López, “Acoustic detection of bearing faults through fractional harmonics lock-in amplification,” *Mechanical Systems and Signal Processing*, vol. 185, 2023, doi: 10.1016/j.ymssp.2022.109740.

[18] D. Romahadi, M. Fitri, D. Feriyanto, I. Hidayat, and M. Imran, "Applying Bayesian networks in making intelligent applications for static and dynamic unbalance diagnosis," *IAES International Journal of Artificial Intelligence*, vol. 13, no. 1, pp. 174–184, 2024, doi: 10.11591/ijai.v13.i1.pp174-184.
[19] B. Gong, Z. Zhang, C. Feng, J. Yin, N. Li, and D. Wang, "Experimental investigation of characteristics of tip leakage vortex cavitation-induced vibration of a pump," *Annals of Nuclear Energy*, vol. 192, 2023, doi: 10.1016/j.anucene.2023.109935.
[20] W. Liu and J. Yu, "Densely connected semi-Bayesian network for machinery fault diagnosis with non-ideal data," *Mechanical Systems and Signal Processing*, vol. 202, 2023, doi: 10.1016/j.ymssp.2023.110678.
[21] P. G. Machado, C. d. O. Ribeiro, and C. A. O. d. Nascimento, "Risk analysis in energy projects using Bayesian networks: a systematic review," *Energy Strategy Reviews*, vol. 47, 2023, doi: 10.1016/j.esr.2023.101097.
[22] L. Wang, H. Cao, Z. Ye, and H. Xu, "Bayesian large-kernel attention network for bearing remaining useful life prediction and uncertainty quantification," *Reliability Engineering and System Safety*, vol. 238, 2023, doi: 10.1016/j.ress.2023.109421.
[23] P. Nivesrangsan and D. Jantarajirojkul, "Bearing fault monitoring by comparison with main bearing frequency components using vibration signal," in *Proceedings of 2018 5th International Conference on Business and Industrial Research: Smart Technology for Next Generation of Information, Engineering, Business and Social Science, ICBIR 2018*, 2018, pp. 292–296, doi: 10.1109/ICBIR.2018.8391209.
[24] R. R. Shubita, A. S. Alsadeh, and I. M. Khater, "Fault detection in rotating machinery based on sound signal using edge machine learning," *IEEE Access*, vol. 11, pp. 6665–6672, 2023, doi: 10.1109/ACCESS.2023.3237074.
[25] D. Romahadi, A. A. Luthfie, and L. B. Desti Dorion, "Detecting classifier-coal mill damage using a signal vibration analysis," *Sinergi*, vol. 23, no. 3, p. 175, 2019, doi: 10.22441/sinergi.2019.3.001.
[26] J. Wang, L. Chen, Y. Wang, and L. Wei, "Vibration analysis and fault diagnosis of coupling misalignment," *2020 5th International Conference on Mechanical, Control and Computer Engineering, ICMCCE 2020*, pp. 452–455, 2020, doi: 10.1109/ICMCCE51767.2020.00105.
[27] A. A. F. Ogaili, A. A. Jaber, and M. N. Hamzah, "Wind turbine blades fault diagnosis based on vibration dataset analysis," *Data in Brief*, vol. 49, 2023, doi: 10.1016/j.dib.2023.109414.

BIOGRAPHIES OF AUTHORS

Wiwit Suprihatiningsih holds a Doctor of Philosophy (Ph.D.) in Mechanical Engineering from Universiti Tun Hussein Onn Malaysia, Malaysia. She also holds a Master of Science (M.Sci.) degree in Mathematics Science. Since October 2015, she has served as a permanent instructor at Universitas Mercu Buana in Jakarta, Indonesia. Her research focuses on the application of mathematics in the field of mechanical engineering. Her findings have been published in numerous journals, both national and international. She can be contacted at email: wiwit.suprihatiningsih@mercubuana.ac.id.

Dedik Romahadi holds a Master of Science (M.Sc.) degree in Mechanical Engineering, which he possesses. His academic pursuits include earning a doctoral degree in mechanical engineering from the Beijing Institute of Technology in Beijing, China. Since August 2018, he has also worked as a permanent lecturer at Universitas Mercu Buana in Jakarta, Indonesia. The research that he is conducting includes signal processing and machine learning. The results of his research have been published in several periodicals, both national and international. He can be contacted at email: dedik.romahadi@mercubuana.ac.id.

Aberham Genetu Feleke received a Ph.D. in Mechanical Engineering from Beijing Institute of Technology, Beijing, China, in 2019. He is currently working as a lecturer at Beijing Institute of Technology. He has three years of post-doctoral research experience and seven years of teaching experience in higher education. He co-authored a book called "Advanced control engineering" and published more than twenty research papers in reputable journals and conferences. His research interests include signal processing, human intention prediction, and human-machine collaboration. He can be contacted at email: abrucag@gmail.com.